Ab Initio Analysis of Water-Assisted Reaction Mechanisms in Amide Hydrolysis

S. Antonczak, M. F. Ruiz-López, and J. L. Rivail*

Contribution from the Laboratoire de Chimie Théorique, URA CNRS 510, Université de Nancy I, BP 239, 54506 Vandoeuvre les Nancy Cedex, France

Received September 20, 1993. Revised Manuscript Received February 18, 1994®

Abstract: The water-assisted hydrolysis of formamide has been studied at the MP3/6-31G**//3-21G *ab initio* level for neutral and H_3O^+-promoted processes. The computations predict an important catalytic effect through O-protonation, in agreement with previous results for the nonassisted reaction. Assistance by a water molecule lowers the free energy barriers of the neutral and the acid-promoted reactions, but the effect is especially large in the second case. The influence of electrostatic interactions with the bulk is discussed using a continuum model to represent the liquid. Substantial modifications of the transition-state geometries are predicted, but the average change in the activation barriers is rather small.

I. Introduction

The hydrolysis of amides is a reaction of primary importance, in particular because it is used as a model for the cleavage of peptide bonds in living systems. It involves an acyl-transfer process to water which may be schematically represented as shown in Scheme 1. In spite of the fundamental role played by this reaction in many biochemical processes, its mechanism has not been completely elucidated. For instance, several mechanisms have been proposed for the hydrolysis reaction of some peptides catalyzed by carboxypeptidase A[1,2] or thermolysin,[2] two common zinc peptidases. Nonenzymatic reactions have received less attention, but the current understanding of the mechanisms of H_3O^+- and OH^--promoted amide hydrolysis has been recently reviewed.[3]

Though many experimental data are available, only a few theoretical computations have been devoted to the study of the amide hydrolysis mechanism. The reaction of ammonia and formic acid to yield formamide and water (i.e., the reverse process of formamide hydrolysis) has been studied by Oie et al.[4] and by Jensen et al.[5] The neutral and acid- or base-promoted hydrolysis of formamide has been investigated by Krug et al.[6] The cleavage of peptides by carboxypeptidase A has been examined using *ab initio* and AM1 computations.[7] Hydrolysis of β-lactams has been also considered by semiempirical approaches[8] including a study of the surroundings effect on the reaction.[9]

In their study, Krug et al.[6] analyzed in detail the reaction pathways for the reaction of formamide with a single water molecule for the neutral reaction and for the reaction catalyzed by H_3O^+ (for both oxygen and nitrogen protonation) or by OH^-. These authors have reported an interesting analysis of the reactions using Bader's atoms in molecules approach[10] at the MP2/6-31G**//4-31G[11] level of computation. It has been shown that N-protonated formamide is more easily hydrolyzed than O-protonated formamide, although the later species is more stable by 14 kcal·mol^{-1}. In fact, N-protonation is the essential step in crossing the activation barrier in both reactions. The transition state may be represented as shown in Chart 1. The transition state leads to formation of a reaction intermediate (see Chart 2) which consists of a hydrogen-bonded complex between an ammonia molecule and formic acid in the case of the neutral reaction and a complex with the CN bond partially broken in the case of the O-protonated reaction. A further energy barrier must be crossed to yield the products, but in both cases it is lower than the first barrier, especially in the case of the neutral reaction.

Scheme 1

A stepwise mechanism can be also considered for the neutral reaction. In the first step, a water molecule hydrates the carbonyl double bond to give a dialcohol reaction intermediate RR'N–$C(OH)_2R''$. In the second step, a proton is transferred from one OH to the nitrogen atom, and simultaneously the NC bond is broken. This mechanism appears to be energetically competitive with the nonpromoted concerted one.[4,5]

* Abstract published in *Advance ACS Abstracts*, April 1, 1994.

(1) Valle, B. L.; Galdes, A.; Auld, D. S.; Riordan, J. F. In *Metal Ions in Biology*; Spiro, T. G., Ed.; Wiley: New York, 1983; Vol. 5, p 25. Rutter, W. J.; Gardell, S. J.; Roczniak, S.; Hilvert, D.; Sprang, S.; Fletterick, R. J.; Craik, C. S. *Protein Eng.* **1987**, 257. Christianson, D. W.; Lipscomb, W. N. *Acc. Chem. Res.* **1989**, *22*, 62. Breslow, R.; Wernick, D. L. *Proc. Natl. Acad. Sci. U.S.A.* **1977**, *74*, 1303. Breslow, R.; Chin, J.; Hilvert, D.; Trainor, G. *Proc. Natl. Acad. Sci. U.S.A.* **1983**, *80*, 4385.

(2) Matthews, B. W. *Acc. Chem. Res.* **1988**, *21*, 333.

(3) Brown, R. S.; Bennet, A. J.; Slebocka-Tilk, H. *Acc. Chem. Res.* **1992**, *25*, 481.

(4) Oie, T.; Loew, G. H.; Burt, S. K.; Binkley, J. S.; MacElroy, R. D. *J. Am. Chem. Soc.* **1982**, *104*, 6169.

(5) Jensen, J. H.; Baldridge, K. K.; Gordon, M. S. *J. Phys. Chem.* **1992**, *96*, 8340.

(6) Krug, J. P.; Popelier, P. L. A.; Bader, R. F. W. *J. Phys. Chem.* **1992**, *96*, 7604.

(7) Alex, A.; Clark, T. *J. Comput. Chem.* **1992**, *13*, 704.

(8) Petrongolo, C.; Ranghino, G.; Scordamaglia, R. *Chem. Phys.* **1980**, *45*, 279. Petrongolo, C.; Ranghino, G. *Theor. Chim. Acta* **1980**, *54*, 239. Petrongolo, C.; Pescatori, E.; Ranghino, G.; Scordamaglia, R. *Chem. Phys.* **1980**, *45*, 291. Frau, J.; Donoso, J.; Muñoz, F.; García Blanco, F. *J. Comput. Chem.* **1991**, *13*, 681.

(9) Rivail, J.-L.; Loos, M.; Théry, V. In *Trends in Ecological Physical Chemistry*; Bonati, L., Cosentino, U., Lasagni, M., Moro, G., Pitea, D., Schiraldi, A., Eds.; Elsevier: Amsterdam, 1993; pp 17–26. Frau, J.; Donoso, J.; Muñoz, F.; García Blanco, F. *J. Comput. Chem.* **1993**, *14*, 1545.

(10) Bader, R. F. W. *Atoms In Molecules—A Quantum Theory*; Oxford University Press: Oxford, U.K., 1990. Bader, R. W. F. *Chem. Rev.* **1991**, *91*, 893.

(11) The computational level notation B//A used in this paper means that the molecular energy is computed at level B using optimized geometries at level A. The references for the atomic orbital basis sets cited in the present work are as follows: Binkley, J. S.; Pople, J. A.; Hehre, W. J. *J. Am. Chem. Soc.* **1980**, *102*, 939 (for 3-21G). Hehre, W. J.; Ditchfield, R.; Pople, J. A. *J. Chem. Phys.* **1972**, *56*, 2257 (for 4-31G and 6-31G). Hariharan, P. C.; Pople, J. A. *Theor. Chim. Acta* **1973**, *28*, 213. Francl, M. M.; Pietro, W. J.; Hehre, W. J.; Binkley, J. S.; Gordon, M. S.; DeFrees, J. D.; Pople, J. A. *J. Chem. Phys.* **1982**, *77*, 3654 (for 6-31G* and 6-31G**). The usual * and ** notations hold for polarization functions on first-row atoms only or in both first-row and hydrogen atoms. For Møller–Plesset energy expressions, see, for instance: Szabo, A.; Ostlund, N. S. In *Modern Quantum Chemistry: Introduction to Advanced Electronic Structure Theory*; Macmillan: New York, 1986; Chapter 6.

0002-7863/94/1516-3912$04.50/0

Chart 1

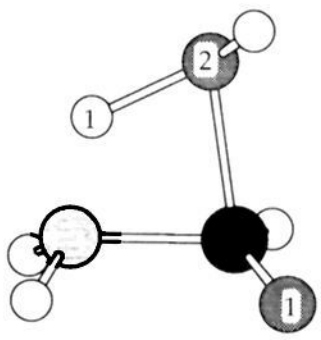

Chart 2

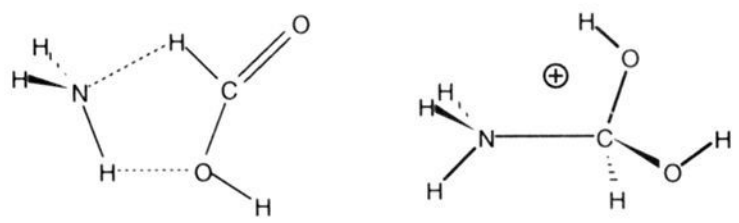

Neutral O-protonated

These reaction mechanisms have been obtained for an isolated reactive system. However, the effect of interactions with the solvent is probably important and deserves further study. Indeed, in addition processes to double bonds, the presence of an ancillary water molecule in the reaction often lowers the height of the transition barriers[12-17] through a bifunctional catalysis mechanism. Assistance by other molecular species has been also demonstrated.[18,19] Such a "water-assisted" reaction mechanism has not been yet envisaged in the case of amide hydrolysis, although it has been suggested,[6] and it is our aim in this paper to theoretically investigate it.

Apart from these specific solvent effects, one may expect that interactions with the bulk also modify the energetics of the processes. Solute–solvent electrostatic interactions are well known to play a role in the kinetics of several reactions.[20] Their effect on the hydrolysis mechanism of amides has not been analyzed in detail, although it can be substantial, since in proton-transfer processes the total dipole moment of the system is expected to change along the reaction coordinate. The use of continuum models has allowed examination of the electrostatic solvent effect on the mechanisms of several reactions.[21-25] In this work, we investigate the role of electrostatic interactions in the amide hydrolysis reaction.

We first consider the mechanism of neutral amide hydrolysis, since understanding it is important in analyzing the role of the catalyst in promoted reactions. The concerted mechanism only will be discussed since in the stepwise reaction the effect of an ancillary water molecule is expected to be quite similar to that obtained for the hydration of other carbonyl bonds.[17] Besides, the first step of this mechanism is unlikely for catalyzed processes, which are the most interesting ones from the point of view of peptide hydrolysis modeling. The H_3O^+-promoted reaction is studied afterwards. Our attention is focused on the first step of the reactions, i.e., the concerted protonation of N and hydroxylation of C. This is the rate-limiting step for the present reactions, as already mentioned, and the subsequent reaction steps are essentially the same as those found in the nonassisted mechanism, as shown below. Finally, the electrostatic solvent effect on the structure of reagents and transition states and on the reaction energetics is discussed.

II. Method of Computation

Because of the presence of two water molecules in the reagents, a number of stable hydrogen-bonded molecular species may be formed. This leads to a rather complex potential energy surface to which several low vibrational frequencies are associated, rendering the location of the transition states difficult. For this reason, the computational scheme used is relatively simple. The geometries have been fully optimized at the RHF/3-21G[11] level. Single point computations have then been carried out at the 6-31G** [11] level. Correlation energy has been computed through the Møller–Plesset perturbation method.[11] It has been shown[4] that the difference in correlation energies obtained at the third or fourth order from those obtained at the second order is nearly constant for the neutral nonassisted reaction with the 6-31G** basis set. This has been also assumed[18] in the case of assisted processes. We have computed MP2 and MP3 corrections. Though limitation to MP3 is somewhat arbitrary, it has been included here to allow comparison with previous works and to get a better estimate of the free energies of activation (MP4 calculations have not been carried out because of the other limitations of the model, which introduce some uncertainties which are probably larger than the improvement introduced by these refined computations).

Such a simple computational scheme always has to be employed with some caution, in particular, the use of the 3-21G basis set for geometry optimizations. The following remarks should be kept in mind: (1) hydrogen bond strength is probably overestimated;[12] (2) formamide–water potential surfaces being rather flat, the optimized geometries are expected to be quite basis set dependent, in particular for polarization functions;[26] (3) though the 3-21G basis set predicts a planar geometry for formamide, in agreement with accurate *ab initio* calculations,[27] it overestimates its stability. One may illustrate this by evaluating the total energy difference of two formamide conformations: (a) the 3-21G optimized planar geometry and (b) a nonplanar structure deduced from the previous by changing the H_NNCO dihedral angles (H_N = hydrogen atoms bonded to N). For instance, assuming angles of 30° and 150° (typical values for the TS structures considered below), one gets $E_b - E_a$ = 11.47 kcal·mol^{-1} at the 3-21G level and 7.11 kcal·mol^{-1} at the MP2/6-31G** level.

However, for the purposes of this paper, this computational scheme may be considered as suitable. One argument justifying this choice arises from the analysis of previous results for related reactions. The activation barrier for nonassisted formamide hydrolysis has been computed at different computational levels.[4,5] Using 3-21G geometries, one obtains 63.1 and 42.0 kcal·mol^{-1} by 6-31G** and MP2/6-31G** single point calculations, respectively.[4] These values change slightly when the more accurate 6-31G* [11] geometries are employed (62.0 and 42.2 kcal·mol^{-1}, respectively).[5] Besides, one should consider that the main limitation of

(12) Williams, I. H. *J. Am. Chem. Soc.* **1987**, *109*, 6299. Williams, I. H.; Spangler, D.; Femec, D. A.; Maggiora, G. M.; Schowen, R. L. *J. Am. Chem. Soc.* **1983**, *105*, 31.

(13) Lledós, A.; Bertrán, J. *Tetrahedron Lett.* **1981**, *22*, 775. Lledós, A.; Bertrán, J.; Ventura, O. N. *Int. J. Quantum Chem.* **1986**, *30*, 467. Ventura, O. N.; Lledós, A.; Bonaccorsi, R.; Bertrán, J.; Tomasi, J. *Theor. Chim. Acta* **1987**, *72*, 175. Clavero, C.; Duran, M.; Lledós, A.; Ventura, O. N.; Bertrán, J. *J. Comput. Chem.* **1986**, *8*, 81.

(14) Nguyen, M. T.; Hegarty, A. F. *J. Am. Chem. Soc.* **1983**, *105*, 3811. Nguyen, M. T.; Hegarty, A. F. *J. Am. Chem. Soc.* **1984**, *106*, 1552. Nguyen, M. T.; Ha, T.-K. *J. Am. Chem. Soc.* **1984**, *106*, 599.

(15) Ruelle, P.; Kesserling, U. W.; Ho, N.-T. *J. Am. Chem. Soc.* **1986**, *108*, 371. Ruelle, P. *J. Am. Chem. Soc.* **1987**, *109*, 1722.

(16) Buckingham, A. D.; Handy, N. C.; Rice, J. E.; Somasundram, K.; Dijkgraaf, C. *J. Comput. Chem.* **1986**, *7*, 283.

(17) Ventura, O. N.; Coitiño, E. L.; Lledós, A.; Bertran, J. *J. Comput. Chem.* **1992**, *13*, 1037.

(18) Oie, T.; Loew, G. H.; Burt, S. K.; MacElroy, R. D. *J. Am. Chem. Soc.* **1983**, *105*, 2221.

(19) Ruelle, P. *J. Comput. Chem.* **1987**, *8*, 158. Clavero, C.; Duran, M.; Lledós, A.; Ventura, O. N.; Bertrán, J. *J. Am. Chem. Soc.* **1986**, *108*, 998. Clavero, C.; Duran, M.; Lledós, A.; Ventura, O. N.; Bertrán, J. *J. Comput. Chem.* **1986**, *8*, 81. Nguyen, K. A.; Gordon, M. S.; Truhlar, D. G. *J. Am. Chem. Soc.* **1991**, *113*, 1596.

(20) Reichardt, C. *Solvent and Solvent Effects in Organic Chemistry*; VCH: Weinheim, 1988.

(21) Rivail, J.-L. In *Chemical Reactivity in Liquid: Fundamental Aspects*; Moreau, M., Turq, P., Eds.; Plenum Press: New York, 1988; pp 187–196. Papalardo, R. R.; Sánchez-Marcos, E.; Ruiz-López, M. F.; Rinaldi, D.; Rivail, J.-L. *J. Am. Chem. Soc.* **1993**, *115*, 3722. Ruiz-López, M. F.; Assfeld, X.; García, J. I.; Mayoral, J. A.; Salvatella, L. *J. Am. Chem. Soc.* **1993**, *115*, 8780. Assfeld, X.; Sordo, J. A.; González, J.; Ruiz-López, M. F.; Sordo, T. L. *J. Mol. Struct. (THEOCHEM)* **1993**, *287*, 193.

(22) Tucker, S. C.; Truhlar, D. G. *Chem. Phys. Lett.* **1989**, *157*, 164. Cramer, C. J.; Truhlar, D. G. *J. Am. Chem. Soc.* **1992**, *114*, 8794.

(23) Tapia, O. In *Theoretical Models of Chemical Bonding*: Maksic, Z. B., Ed.; Springer: Berlin, 1991; Part IV, p 435.

(24) Solà, M.; Lledós, A.; Durán, M.; Bertrán, J.; Abboud, J. L. M. *J. Am. Chem. Soc.* **1991**, *113*, 2873. Tortonda, F. R.; Pascual-Ahuir, J. L.; Silla, E.; Tuñon, I. *J. Phys. Chem.* **1993**, *97*, 11087.

(25) Tomasi, J.; Bonnacorsi, R.; Cammi, R.; Olivares del Valle, F. J. *J. Mol. Struct.* (THEOCHEM) **1991**, *234*, 401.

(26) Jasien, P. G.; Stevens, W. J. *J. Chem. Phys.* **1986**, *84*, 3271.

(27) Kwiatkowski, J. S.; Leszczynski, J. *J. Mol. Struct.* **1993**, *297*, 277.

Chart 3

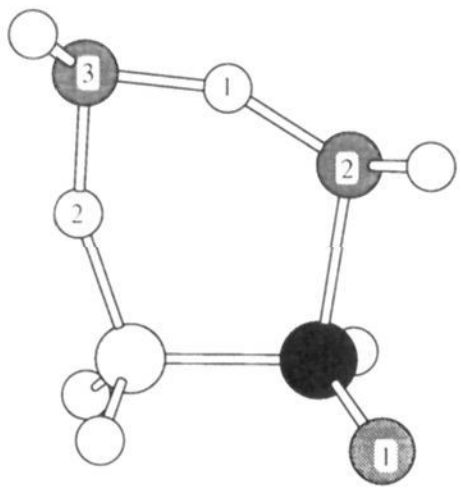

our calculations is due to the rough representation of the interactions with the molecular surroundings and that the present work, whose aim is to explore some possible reaction mechanisms not yet studied, is intended to describe the main features of the reaction as well as the structure of the transition states and reaction intermediates. It is clear that an accurate evaluation of the energetics of the process would require not only a higher computational level but also the use of a more elaborated model to represent the liquid.[28]

The average effect of the bulk solvent on the hydrolysis reaction is examined using a continuum model described previously.[29] The solute is assumed to be placed into a cavity created in a dielectric continuum. Due to the charge distribution of the solute, the continuum is polarized and creates an electric field inside the cavity that is computed using a multipole expansion of the solute's charge distribution. The free energy of solvation can then be written as a sum of multipole contributions which, in general, converges quite rapidly (in our computations, the multipole expansion has been performed up to the sixth order). The corresponding electrostatic interaction is included in the solute's Hamiltonian, and the Hartree–Fock equations are solved, allowing computation of polarization effects on the solute's electronic cloud and on its equilibrium geometry, usually different from the gas-phase structure. The shape of the cavity is a three-axes ellipsoid adapted to the shape of the solute by an algorithm described previously.[29b] This allows efficient geometry optimization for solvated molecules using analytical gradients.[29b] Second derivatives of the solvation energy are computed numerically. This allows the structure of the solvated transition states to be obtained within the electrostatic continuum model. TS structures have been located by inspecting the energy surface given by the intrinsic energy of the molecule plus the electrostatic free energy of solvation, which is the only solvation term assumed to change in the geometry optimization process.

Location of the TS in this way assumes that the solvent follows adiabatically the changes in the geometry and electronic distribution of the solute along the reaction path. Two extreme situations can be considered. In the case of a nonpolar solvent, the dielectric permittivity arises mainly from the polarization of the electrons, and the response of the medium to changes in the solute's geometry and electronic distribution may be assumed to be instantaneous. In a polar medium, the nuclear relaxation of the solvent molecules has to be considered, too, and a rigorous study of a chemical reaction would require one to account for the dynamics of the whole system. In our work, we shall assume that the reaction field can be still approximated by using the static dielectric permittivity of the solvent. Two media have been considered with dielectric permittivities corresponding to a nonpolar solvent ($\epsilon = 2.0$) and water ($\epsilon = 78.4$) so that our results can be used as lower and upper bounds for the electrostatic solvent effect.

Computations have been carried out with the program Gaussian 92[30] using the SCRFPAC package[31] for the studies on electrostatically solvated systems in a continuum. The transition states (TS) have been located using Schlegel's algorithm[32] and characterized by computing the Hessian matrix and verifying that it has a single negative eigenvalue.

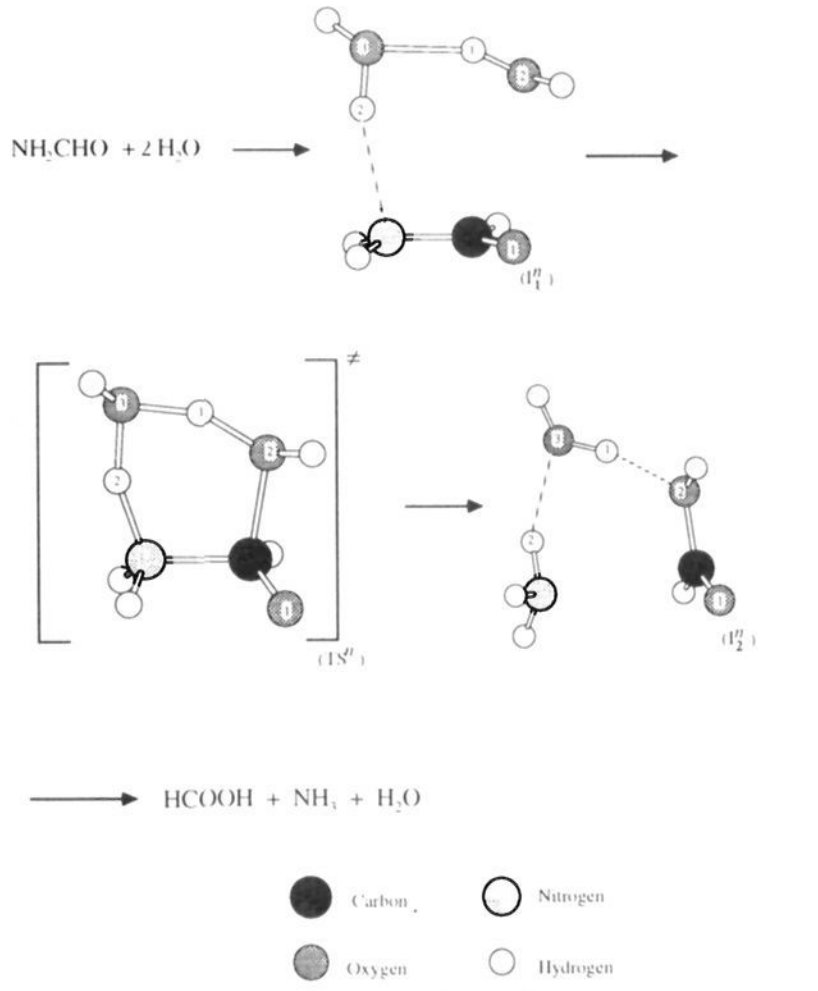

Figure 1. Neutral water-assisted hydrolysis of formamide. Computed structures at the RHF/3-21G level.

III. Results and Discussion

A. Molecular Structures. Neutral Reaction. We have inspected the potential energy surface in the neighborhood of a six-membered ring conformation of the type shown in Chart 3, looking for possible stationary points. Though strictly speaking we do not follow a reaction coordinate, the eigenvector of the negative Hessian matrix eigenvalue has been used to interpret the TS structures obtained below. We neglect the interactions with other water molecules. For instance, hydrogen bonding with the carbonyl would modify the neutral mechanism slightly: its effect is expected to go in the same direction as O-protonation but to be less intense. The computations predict the formation of a prereactive hydrogen-bonded complex (hereafter called reaction intermediate I_1^n) between a hydrogen atom of the water dimer and the nitrogen atom of formamide. A transition state has been located for a six-membered ring structure (hereafter called TS^n). The reaction proceeds to yield ammonia and formic acid via the formation of another reaction intermediate (hereafter called I_2^n), which can be regarded as a hydrogen-bonded complex between these molecules and a water molecule. The predicted reaction step structures are represented in Figure 1. The corresponding geometrical parameters and total energies are summarized in Table 1. Mayer bond indices[33] and net atomic charges (obtained by a Mulliken population analysis) are compiled in Table 2.

(i) Intermediate I_1^n. As shown in Table 1, the reaction intermediate I_1^n corresponds to a weakly N-hydrogen-bonded

(28) Field, M. J.; Bash, P. A.; Karplus, M. *J. Comput. Chem.* **1990**, *11*, 700. Wesolowski, T. A.; Warshel, A. *J. Phys. Chem.* **1993**, *97*, 8050. Stanton, R. V.; Hartsough, D. S.; Merz, K. M., Jr. *J. Phys. Chem.* **1993**, *97*, 11868.

(29) (a) Rinaldi, D.; Ruiz-López, M. F.; Rivail, J.-L. *J. Chem. Phys.* **1983**, *78*, 834. (b) Rinaldi, D.; Rivail, J. L.; Rguini, N. *J. Comput. Chem.* **1992**, *13*, 675.

(30) Frish, M. J.; Trucks, G. W.; Head-Gordon, M.; Gill, P. M. W.; Wrong, M. W.; Foresman, J. B.; Johnson, B. G.; Schlegel, H. B.; Robb, M. A.; Reprogle, E. S.; Gomperts, R.; Andres, J. L.; Raghavachari, K.; Binkley, J. S.; Gonzales, C.; Martin, R. L.; Fox, D. J. Defrees, D. J.; Baker, J.; Stewart, J. J. P.; Pople, J. A. *Gaussian 92*; Carnegie-Mellon Quantum Chemistry Publishing Unit: Pittsburgh, PA, 1992.

(31) Rinaldi, D.; Pappalardo, R. R. *SCRFPAC*; Quantum Chemistry Program Exchange: Indiana University, Bloomington, IN, 1992; Program No. 622.

(32) Schlegel, H. B. *J. Comput. Chem.* **1982**, *3*, 214.

(33) Mayer, I. *Chem. Phys. Lett.* **1983**, *97*, 270.

Table 1. Geometrical Parameters (Bond Distances, Bond Angles, and Dihedral Angles in Å and deg) for the Neutral Water-Assisted Hydrolysis of Formamide (See Figure 1) Obtained at the RHF/3-21G level and Total Energies (in au) at Several Computational Levels[a]

	formamide	water dimer	I_1^n	TS^n	I_2^n
		Geometrical Parameters			
CN	1.353		1.382	1.572	2.839
CO_1	1.212		1.209	1.239	1.195
CO_2			2.749	1.674	1.375
$O2H_1$		0.973	0.975	1.205	1.883
O_3H_1		1.825	1.796	1.190	0.973
O_3H_2		0.967	0.973	1.190	1.981
NH_2			2.109	1.298	1.008
O_1CN	125.32		123.36	115.18	111.48
O_2CN			107.98	98.85	89.95
H_1O_2C			85.26	113.31	119.48
$O_3H_1O_2$		175.92	156.48	153.58	163.80
$H_2O_3H_1$		110.03	91.04	86.72	83.23
O_3H_2N			165.13	158.34	158.05
H_2NC			100.18	109.16	93.03
H_1O_2CN			25.42	0.16	−32.65
$O_3H_1O_2C$			−16.59	−1.70	57.75
$H_2O_3H_1O_2$		−59.91	6.50	2.20	−24.01
$NH_2O_3H_1$			4.69	−2.95	−4.59
H_2NCO2			−19.36	−0.25	24.66
$H_NNCH'_N$	180.0		151.16	117.79	127.58
		Total Energies			
3-21G	−167.984 900	−151.189 404	−319.186 604	−319.137 385	−319.188 038
6-31G**//3-21G	−168.939 675	−152.052 455	−320.995 999	−320.901 323	−320.993 914
MP2/6-31G**//3-21G	−169.420 470	−152.449 180	−321.879 504	−321.817 900	−321.876 375
MP3/6-31G**//3-21G	−169.429 344		−321.899 218	−321.828 043	−321.895 827

[a] Values obtained for the water molecule are d_{OH} = 0.967 Å, HOH = 107.68°, E = −75.585 960 au (RHF/3-21G//3-21G), E = −76.022 772 au (RHF/6-31G**//3-21G), E = −76.219 313 au (MP2/6-31G**//3-21G), E = −76.225 605 au (MP3/6-31G**//3-21G).

Table 2. Mayer Bond Orders[33] and Mulliken Net Atomic Charges for the Neutral Water-Assisted Hydrolysis of Formamide (See Figure 1) Obtained at the RHF/6-31G**//3-21G Level[a]

	formamide	water dimer	I_1^n	TS^n	I_2^n
		Bond Orders			
CN	1.069		0.987	0.689	0.015
CO_1	1.823		1.824	1.646	1.895
CO_2			0.026	0.429	0.906
O_2H_1		0.801	0.793	0.366	0.043
O_3H_1		0.064	0.075	0.395	0.804
O_3H_2		0.863	0.810	0.410	0.063
NH_2			0.044	0.356	0.843
		Net Atomic Charges			
C	0.567		0.584	0.704	0.672
N	−0.733		−0.786	−0.848	−0.880
O_1	−0.575		−0.576	−0.694	−0.537
O_2		−0.747	−0.755	−0.811	−0.657
O_3		−0.687	−0.719	−0.832	−0.726
H_1		0.388	0.390	0.515	0.397
H_2		0.361	0.386	0.507	0.327

[a] Values for water are B_{OH} = 0.877, q_O = −0.683, q_H = 0.341.

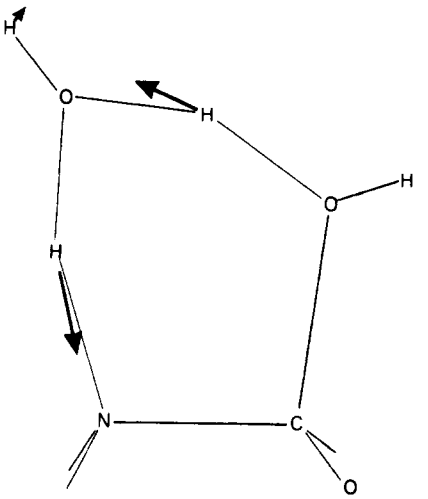

Figure 2. Schematic representation of the Hessian matrix eigenvector components with negative eigenvalue at the TS geometry in the neutral water-assisted mechanism.

complex between the water dimer and the formamide molecule. Due to this interaction, the CN bond is lengthened by 0.029 Å, and nitrogen pyramidalization occurs (as illustrated through the variation of the $H_NN\,CH_{N'}$ angle). The carbonyl CO bond length is slightly smaller in the complex than in free formamide, which is obtained for N-protonated formamide,[6] too.

In the nonassisted mechanism reported previously,[4-6] the presence of a similar hydrogen-bonded complex has not been pointed out. We have carried out a set of computations to check the possible formation of a N-bonded formamide–water complex, but no energy minimum has been found at the present computational level. This is in agreement with extended double-ζ computations.[26]

The formation of such a complex requires pyramidalization of the nitrogen atom and a electron delocalization loss. If the donor character of the protic species is large enough, then the stablization energy due to hydrogen bonding could compensate the energy spent to modify the nitrogen hybridization and the complex could be formed. Due to cooperative effects,[34] the hydrogen atoms of the H-acceptor water molecule in the water dimer have a greater ability to form hydrogen bonds than those of the water monomer. This explains, at least partially, the difference in water–formamide and water dimer–formamide interactions.

(ii) Transition State TS^n. The structure of TS^n is a six-membered ring not far from planarity that involves a concerted proton-transfer mechanism. This is schematized in Figure 2, where we have represented the eigenvector corresponding to the negative Hessian matrix eigenvalue. The water molecule whose oxygen atom interacts with the amidic carbon is deprotonated, the other water molecule being the acceptor species. Simultaneously, the second water molecule loses a proton, which is transferred to the nitrogen atom. Note in Tables 1 and 2 that the CN bond is substantially weakened, as shown by the large

(34) Bertrán, J.; Ruiz-López, M. F.; Rinaldi, D.; Rivail, J.-L. *Theor. Chim. Acta* **1992**, *84*, 181 and references cited therein.

increase of its bond length (0.19 Å with respect to I_1^n) and the decrease of its bond order (0.298 with respect to I_1^n).

As shown in Table 1, the three OH distances in the ring have close values. The forming O_3H_1 bond is slightly shorter and stronger than the breaking O_2H_1 bond. Hence, in the transition state, the water–water proton transfer is slightly closer to the final state. The H_2 proton has substantially approached the nitrogen, and the NH_2 bond order is significant.

One may compare the water-assisted TS structure with that obtained in the nonassisted reaction. In the latter, the lengths of the bonds being broken (CN) or formed (CO and NH) are d_{CN} = 1.598 Å, d_{CO} = 1.749 Å, and d_{NH} = 1.220 Å.[4] In the former, the corresponding values are 1.572, 1.674, and 1.298 Å, respectively (see Table 1). Thus, in the water-assisted TS, the cleavage of the amidic CN bond and the proton transfer to N appear to be retardated, in spite of the greater donor character of the water dimer. Conversely, the formation of the CO bond is substantially favored by the presence of an ancillary water molecule. The pyramidalization of the N atom is greater in the water-assisted mechanism TS. This is illustrated by the value of the $H_NNCH_{N'}$ angle, which is 117.8° in the water-assisted TS and 128.1° in the nonassisted TS (this last value is not given in ref 4, but it has been computed in this work after the corresponding TS structure was located). Finally, the carbonyl CO bond length, which increases under TS formation, is greater in the case of the assisted reaction (d_{CO} = 1.239 Å vs d_{CO} = 1.217 Å in the nonassisted reaction), as expected considering the fact that the forming CO bond is shorter.

These values show that the modifications on the TS structure produced by the presence of the ancillary water molecule are complex and cannot be explained by single factors, like geometrical constraints (different in the four-membered and six-membered rings) or hydrogen donor character. Nevertheless, changing the hybridization of N appears to be a key feature. It has been pointed out[35] that nitrogen pyramidalization is accompanied by an increase of the amidic carbon susceptibility to nucleophilic attack, and, in fact, this is observed when both mechanisms are compared. In the nonassisted mechanism, pyramidalization of the nitrogen atom is energetically disfavored and requires a closer approach of the water molecule, rendering the nucleophilic attack at the carbon more difficult than in the two water molecule mechanism.

(iii) Intermediate I_2^n. In the intermediate species I_2^n, the CN bond has been broken: an ammonia molecule and a formic acid molecule are linked through two hydrogen bonds (see Figure 1). The structure of this intermediate is very close to that found in the nonassisted mechanism,[4] except for the presence of the additional water molecule, which merely solvates the ensemble. Hence, the subsequent reaction steps are expected to be almost the same for the assisted and nonassisted mechanisms and will be not analyzed here.

H_3O^+-Promoted Reaction. We shall discuss only the O-protonated case since, as shown before,[6] it is the most stable structure and its formation is assumed to be the first step in the currently favored mechanism for H_3O^+-catalyzed amide hydrolysis.[3,36,37] Thus, we shall assume that the oxygen atom belonging to the amidic carbonyl group is bound to an H_3O^+ group along the reaction path.

The structures of the corresponding optimized reaction intermediates (I_1^p, I_2^p) and transition state (TS^p) are represented in Figure 3. Some geometrical parameters are gathered in Table 3. In Table 4 we summarize the values obtained for the bond orders and Mulliken net atomic charges.

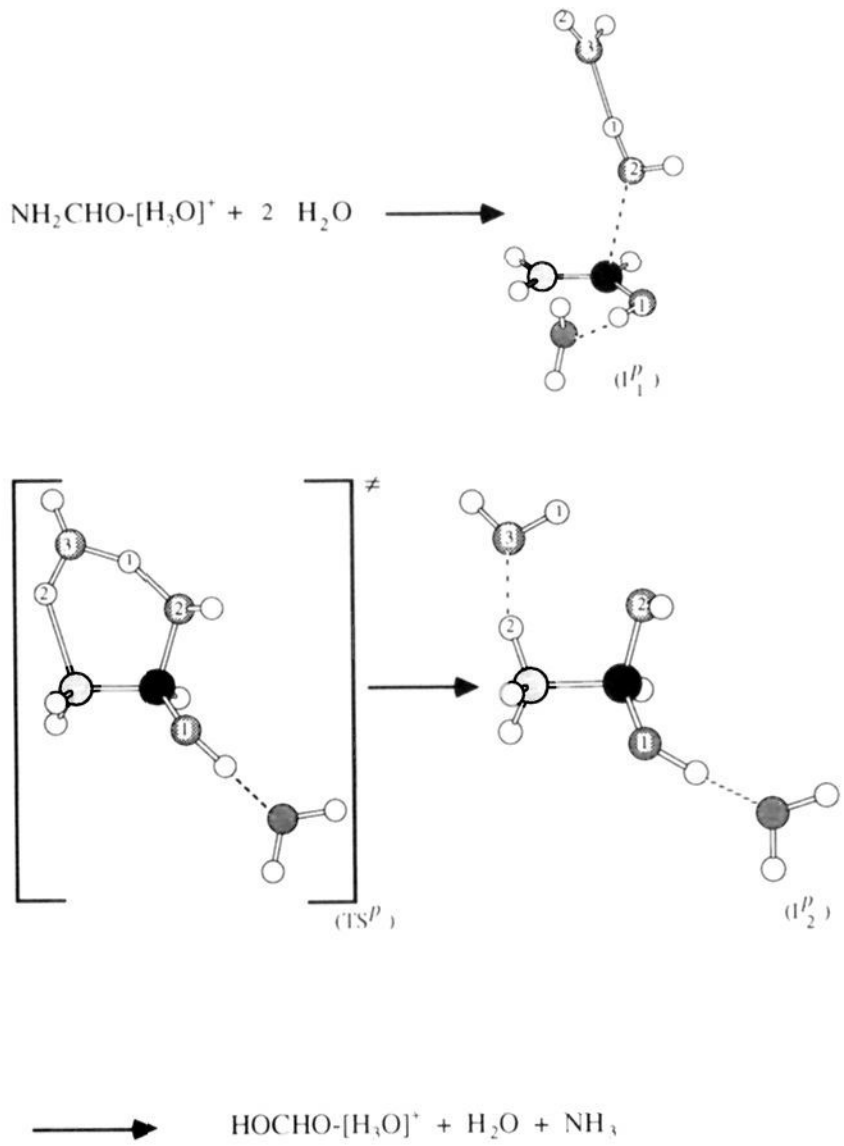

Figure 3. $[H_3O]^+$-promoted water-assisted hydrolysis of formamide. Computed structures at the RHF/3-21G level. See Figure 1 for symbols.

(i) Protonated Formamide. Protonation of the oxygen in formamide induces drastic changes on its geometry. The CO bond length substantially increases and the CN bond length decreases, which may be schematically interpreted by considering that the configuration in Chart 4 is stabilized under O-protonation. Comparison of the values computed for the NC and CO bond orders and for the net N atomic charge in free and protonated formamide supports this interpretation, too.

Due to the large perturbation of the formamide molecule, one may expect substantial changes for the geometries of I_1^p, TS^p, and I_2^p in the catalyzed reaction, as indeed happens.

(ii) Intermediate I_1^p. The weak NH_2 hydrogen bond between formamide and the bifunctional water molecule predicted in the case of the neutral reaction is not found in the case of the acid-catalyzed reaction. Instead, the intermediate I_1^p has a partially formed CO_2 bond. The remarks made before for protonated formamide remain true for I_1^p, i.e., the carbonyl bond length is longer and the CN bond length is shorter than in I_1^n.

(iii) Transition State TS^p. The structure of TS^p exhibits important differences with respect to TS^n. Note, for instance, the changes in CO_1, CO_2, and NH_2 bond lengths. Proton transfer between water molecules is almost complete, whereas proton transfer to the amidic nitrogen has barely started. Accordingly, the oxygen O_3 and the three hydrogen atoms linked to it form an H_3O^+-like species, where most of the positive charge is located.

Another important difference between the TS structures is that, in the promoted reaction, the six-membered ring is not planar (see the angle H_2NCO_2 in Table 3). Indeed, in this reaction, the amino group rotates with respect to the CNO plane, as illustrated in Chart 5a (this rotation being preferred to the clockwise rotation in Chart 5b). Like N-pyramidalization, rotation around CN has been shown[38] to enhance the susceptibility of amides to nucleophilic attack at the carbon atom.

In the computations by Krug et al.[6] for the nonassisted processes, the structure of the TS for the H_3O^+-promoted mechanism was

(35) Wang, Q.-P.; Bennet, A. J.; Brown, R. S. *Can. J. Chem.* **1990**, *68*, 1732. Bennet, A. J.; Wang, Q.-P.; Slebocka-Tilk, H.; Somayaji, V.; Brown, R. S.; Santarsiero, B. D. *J. Am. Chem. Soc.* **1990**, *112*, 6383. Wang, Q.-P.; Bennet, A. J.; Brown, R. S.; Santarsiero, B. D. *J. Am. Chem. Soc.* **1991**, *113*, 5757.

(36) Williams, A. *J. Am. Chem. Soc.* **1976**, *98*, 5645.

(37) Bennet, A. J.; Slebocka-Tilk, H.; Brown, R. S.; Guthrie, J. P.; Jodhan, A. *J. Am. Chem. Soc.* **1990**, *112*, 8497.

Table 3. Geometrical Parameters (Bond Distances, Bond Angles, and Dihedral Angles in Å and deg) for the $[H_3O]^+$-Promoted Water-Assisted Hydrolysis of Formamide (see Figure 3) Obtained at the RHF/3-21G Level and Total Energies (in au) at Several Computational Levels

	NH_2CHO–$[H_3O]^+$	I_1^p	TS^p	I_2^p
		Geometrical Parameters		
CN	1.293	1.302	1.459	1.538
CO_1	1.268	1.290	1.368	1.362
CO_2		2.254	1.485	1.402
O_2H_1		0.986	1.277	2.323
O_3H_1		1.667	1.123	0.967
O_3H_2		0.965	1.000	1.539
NH_2		5.191	1.800	1.064
O_1CN	121.01	122.76	112.75	105.54
O_2CN		103.30	106.98	105.28
H_1O_2C		135.11	113.98	108.85
$O_3H_1O_2$		175.18	153.13	109.76
$H_2O_3H_1$		125.55	101.41	109.50
O_3H_2N		52.95	133.48	162.71
H_2NC		84.88	107.17	107.12
H_1O_2CN		−40.16	−20.53	−40.91
$O_3H_1O_2C$		−151.52	11.24	22.36
$H_2O_3H_1O_2$		−105.60	−1.36	3.94
$NH_2O_3H_1$		−35.88	4.30	7.27
H_2NCO_2		8.85	20.56	40.14
$H_NNCH'_N$	180.0	172.97	122.33	118.35
		Total Energies		
3-21G	−243.975 524	−395.202 111	−395.190 013	−395.210 586
6-31G**//3-21G	−245.338 638	−397.413 896	−397.370 858	−397.409 737
MP2/6-31G**//3-21G	−246.017 757	−398.491 336	−398.465 232	−398.496 632
MP3/6-31G**//3-21G	−246.036 096	−398.521 567	−398.493 370	−398.527 104

Table 4. Mayer Bond Orders[33] and Mulliken Net Atomic Charges for the $[H_3O]^+$-Promoted Water-Assisted Hydrolysis of Formamide (See Figure 3) Obtained at the RHF/6-31G**//3-21G Level

	NH_2CHO–$[H_3O]^+$	I_1^p	TS^p	I_2^p
		Bond Order		
CN	1.381	1.327	0.923	0.776
CO_1	1.332	1.223	1.023	1.030
CO_2		0.055	0.687	0.916
O_2H_1		0.743	0.268	0.017
O_3H_1		0.070	0.446	0.824
O_3H_2		0.850	0.698	0.113
NH_2		0.000	0.119	0.674
		Net Atomic Charges		
C	0.606	0.687	0.721	0.667
N	−0.643	−0.678	−0.826	−0.689
O_1	−0.615	−0.597	−0.710	−0.709
O_2		−0.718	−0.745	−0.661
O_3		−0.733	−0.666	−0.736
H_1		0.446	0.555	0.400
H_2		0.378	0.455	0.481

Chart 4

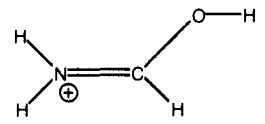

quite similar to that found for the nonpromoted mechanism, except for an increase of the asymmetry in these concerted reactions. This effect is also predicted in our study of the water-assisted mechanism, but it is much larger.

The eigenvector corresponding to the negative eigenvalue of the Hessian matrix is schematically represented in Figure 4. One notices slight differences between this mechanism and the nonpromoted mechanism in Figure 2.

(iv) Intermediate I_2^p. This intermediate is a tetrahedral complex solvated by two water molecules. The CN bond is not broken, as opposed to the neutral reaction, since in this case the interaction between the nucleophilic species NH_3 and the activated carbon atom is larger. Further lengthening of the CN bond is necessary to get the final products, but here again, this part of the reaction is essentially the same as that in the nonassisted mechanism.

Chart 5

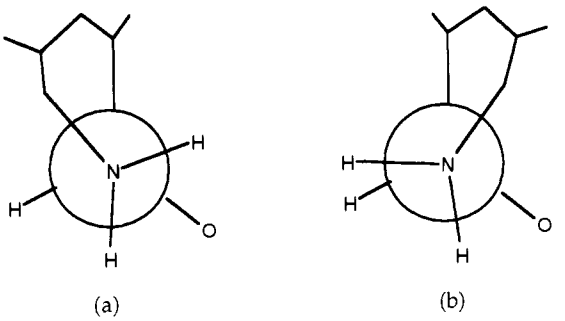

(a) (b)

B. Energetics of the Reactions. In Table 5, we give the relative energies of the reaction species with respect to the separate components for the neutral and H_3O^+-promoted water-assisted mechanisms. The TS relative energies for nonassisted reactions are also given. In Figure 5, the potential energy surfaces are schematized. The shape of the potential energy surface is very different in the neutral and H_3O^+-promoted reactions. The relative energy of the intermediates and transition state with respect to the reagents decreases drastically in the catalyzed reaction. The energy barrier separating the intermediates is substantially smaller in the latter process.

Note that correlation energy modifies the SCF relative energies, stabilizing the intermediates and, above all, the TSs with respect to the reagents. Differences between MP2 and MP3 values for the neutral reaction TS (~7 kcal·mol^{-1}) are comparable to those obtained for the nonassisted process (~6 kcal·mol^{-1}). This difference decreases in the H_3O^+-promoted reaction (~2 kcal·mol^{-1}).

Comparison of relative energies in assisted and nonassisted processes shows that assistance by a water molecule substantially stabilizes the TS species with respect to the reagents. Depending on computational level, the effect reaches 10–16 kcal·mol^{-1} in the neutral reaction and 34–35 kcal·mol^{-1} in the promoted one.

(38) Laidig, K. E.; Bader, R. F. W. *J. Am. Chem. Soc.* **1991**, *113*, 6312.

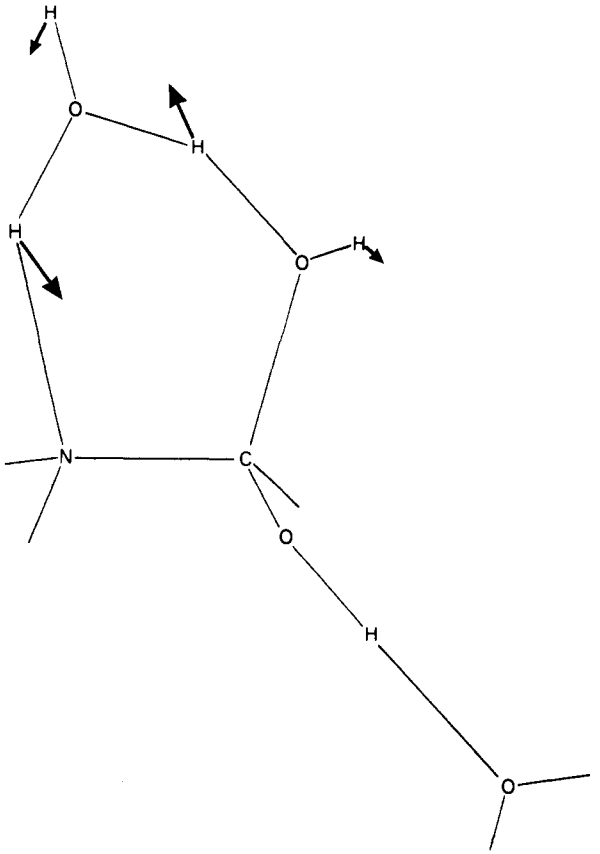

Figure 4. Schematic representation of the Hessian matrix eigenvector components with negative eigenvalue at the TS geometry in the $[H_3O]^+$-promoted water-assisted mechanism.

Table 5. Relative Energies (in kcal·mol^{-1}) of the Water-Assisted Reaction Species with Respect to the Separate Components (Formamide or Formamide–$[H_3O]^+$ and Water)[a]

	RHF/6-31G**// 3-21G	MP2/6-31G**// 3-21G	MP3/6-31G**// 3-21G
	Neutral Mechanism		
I_1^n	−7.39	−12.84	−11.71
TS^n	+52.02	+25.82	32.95
	(+63.3)[b]	(+42.0)[b]	(+48.3)[b]
I_2^n	−6.08	−10.87	−9.58
	$[H_3O^+]$-Promoted Mechanism		
I_1^p	−19.27	−21.94	−21.50
TS^p	+7.72	−5.56	−3.81
	(+38.47)[c]	(+23.75)[c]	(+26.43)[c]
I_2^p	−16.88	−25.26	−24.97

[a] Values in parentheses correspond to nonassisted reactions. [b] Reference 4. [c] This work. See ref 6 for a description of the optimized TS structures using the 4-31G basis set.

In order to obtain free energy variations along the reaction paths, we have computed thermodynamic quantities at 298 °C and 1 atm following standard procedures and using the vibrational frequencies computed at the RHF/3-21G level. The results are summarized in Table 6.

Entropic effects are known to be determining for the reactivity of weakly-bonded complexes[39] since the low vibrational frequencies, inherent to their intermolecular coordinates, lead to large negative values of ΔS that strongly disfavor complex formation. Hence, in assisted mechanisms, reaction intermediates and transition states are expected to be substantially destabilized with respect to the separated reagents. Indeed, the entropic contributions to ΔG in Table 6 are quite large but compare pretty well with calculations for other assisted mechanisms.[17,18] Their value is nearly twice that obtained in the nonassisted processes,[4] which

(39) Hobza, P.; Zahradnik, R. *Top. Curr. Chem.* **1980**, *93*, 53.

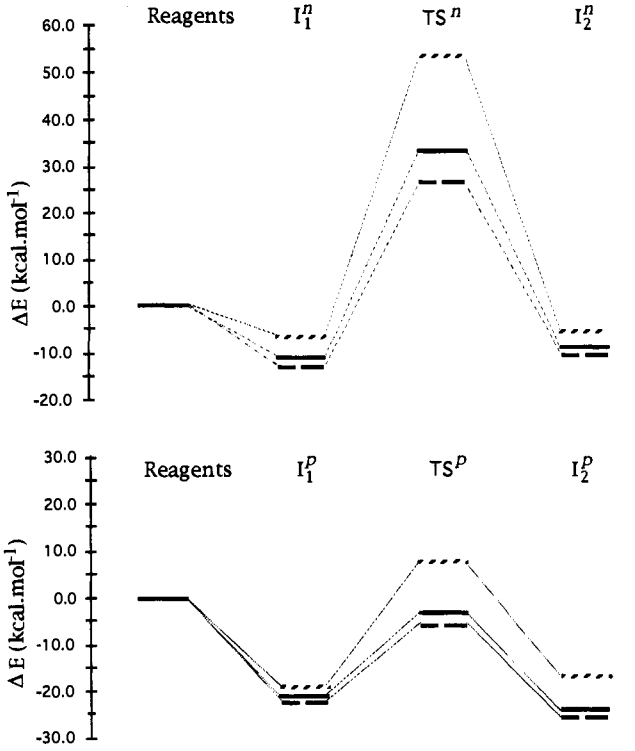

Figure 5. Potential energy surfaces for the water-assisted hydrolysis of formamide: RHF/6-31G**//3-21G (- - -), MP2/6-31G**//3-21G (– –), and MP3/6-31G**//3-21G (—).

Table 6. Energetics for the Water-Assisted Hydrolysis of Formamide (kcal·mol^{-1})[a]

	$\Delta(H-E)$	$-T\Delta S$	ΔG^b RHF	MP2	MP3
		Neutral Mechanism			
I_1^n	5.40	17.61	15.62	10.17	11.30
TS^n	2.01	21.74	75.77	49.57	56.70
	(−0.4)[c]	(11.4)[c]	(74.1)[c]	(53.0)[c]	(59.3)[c]
I_2^n	5.60	17.40	16.92	12.13	13.42
		$[H_3O]^+$-Promoted Mechanism			
I_1^p	6.21	17.47	4.41	1.74	2.18
TS^p	4.15	20.94	32.81	19.53	21.28
	(−0.39)[d]	(11.17)[d]	(49.25)[d]	(34.53)[d]	(37.21)[d]
I_2^p	7.20	19.55	9.87	1.49	1.78

[a] Values in parentheses correspond to nonassisted processes. Enthalpic and entropic contributions are computed using RHF/3-21G vibrational frequencies at 298 K and 1 atm. [b] RHF, MP2, and MP3 holds for RHF/6-31G**//3-21G, MP2/6-31G**//3-21G, and MP3/6-31G**//3-21G computational levels, respectively. [c] Reference 4. [d] This work.

is not surprising because the number of intermolecular coordinates and low frequencies of vibration is larger for the assisted reaction species. Note that in the acid-catalyzed processes, the entropy of activation is slightly smaller than in the corresponding neutral reactions.

All the species have positive ΔG values, contrasting with the ΔE values gathered in Table 5. Accordingly, reaction intermediates I_1^n and I_1^p are both predicted to be unstable at normal temperature and pressure conditions, especially the former. This is also in good agreement with the results obtained in the water-assisted addition of water to formaldehyde.[17] The computed $\Delta G^{\ddagger}$ value for the neutral water-assisted hydrolysis of formamide at the MP2/6-31G**/3-21G level (48.39 kcal·mol^{-1}) is close to that deduced for the neutral ammonia-assisted reaction (50.7 kcal·mol^{-1}) at the same level of calculation.[18] The ΔG for a given species is always smaller in the H_3O^+-catalyzed process. In particular, acid catalysis lowers the activation barrier strongly (by 35 kcal·mol^{-1} at the highest level of computation used here, MP3/6-31G**/3-21G).

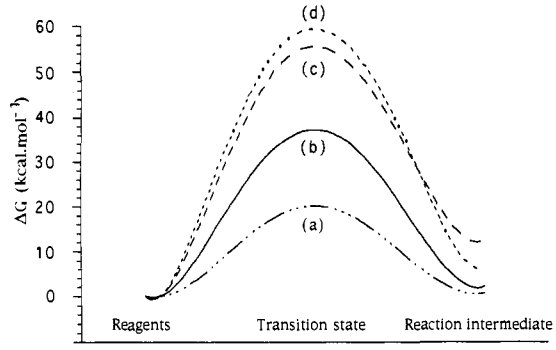

Figure 6. Schematic reaction paths for (a) water-assisted $[H_3O]^+$-promoted, (b) nonassisted $[H_3O]^+$-promoted, (c) water-assisted neutral, and (d) nonassisted neutral mechanisms of formamide hydrolysis at the MP3/6-31G**//3-21G level. See ΔG values in Table 6. ΔG for the intermediates in the nonassisted reactions is 6.71 kcal·mol^{-1} (neutral)[4] and 2.06 kcal·mol^{-1} (promoted, as computed in the present work; see ref 6 for a description of this intermediate at a slightly different computational level).

These results can be compared with those for nonassisted mechanisms. Free energy barriers are given in Table 6, and the schematic reaction paths for the concerted assisted and nonassisted mechanisms are plotted in Figure 6. Only MP3/6-31G**//3-21G results are plotted for simplicity.

At the highest level of computation used here, assistance by an ancillary water molecule substantially lowers the free energy barrier in the acid-catalyzed process (about 50%), but in the neutral reactions it produces a small decrease of the barrier only. Conclusions at the RHF, MP2, and MP3 levels are essentially the same, except that RHF calculations do not predict bifunctional catalysis for the neutral process.

In summary, it appears that two main components have to be considered to explain bifunctional catalysis in amide hydrolysis. On one hand, the ancillary water molecule stabilizes the TS substantially, which results from several factors (geometric, water dimer acidity), but the protonated TS undergoes the largest effect. On the other hand, entropy effects strongly disfavor the assisted mechanisms, although there are not important differences between neutral and promoted processes in this case. Decrease in free energy barriers through bifunctional catalysis is given by the sum of these energetic and entropic contributions: large stabilization occurs in promoted processes, but only small effects are predicted in neutral reactions.

More water molecules could, in principle, be considered in the hydrolysis mechanisms. However, the energy stabilization is expected to be smaller since the participation of the water molecules in the reaction coordinate is unlikely. Conversely, the entropic term $-T\Delta S$ would continue to increase systematically (by about 10 kcal·mol^{-1} per water molecule at 298 K and 1 atm). Hence, these multimolecular processes are not expected in formamide hydrolysis, especially for neutral reactions.

C. Electrostatic Solvent Effects. We now examine the role of electrostatic interactions with the bulk solvent on the reactions described above. Unless otherwise stated, we assume that the relative dielectric permittivity of the liquid is that of water (ϵ = 78.4). Solvation energies have been computed at the MP2/6-31G**/3-21G level (MP3 calculations for solvated systems are too costly and are not expected to modify the conclusions below). Effects on the reagent and TS structures are discussed. It should be reminded that other terms contributing to the free energy of solvation can modify the gas-phase barriers. The total solvation energy should include, in particular, cavitation and dispersion corrections that are important quantities in evaluating activation energies. However, these terms are not expected to influence much the geometry of the stationary points in the free energy surface, and our results for the structures may be regarded with confidence.

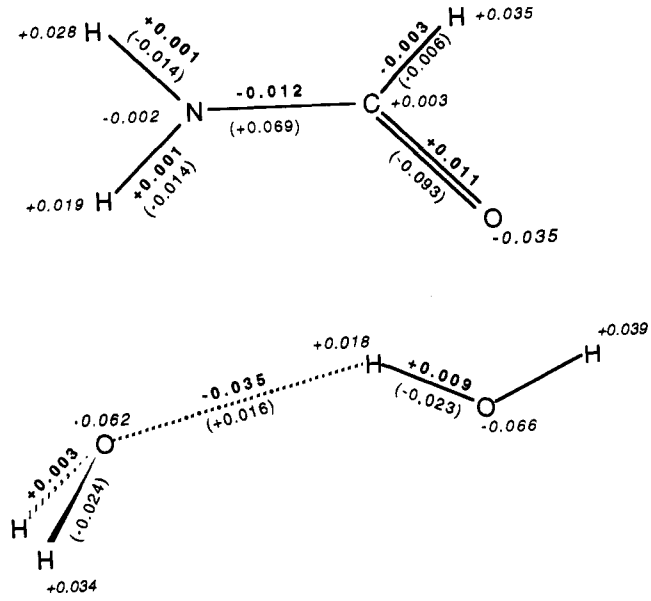

Figure 7. Computed increments of the internal coordinates (bold), bond orders (in parenthesis) and net atomic charges (italic) for formamide and water dimer in going from a vacuum to water solution at the 6-31G**//3-21G level of calculation.

Chart 6

Neutral Reaction. (i) Formamide and Water. First of all, it is interesting to consider how the electrostatic interactions modify the geometry and electronic distribution of the reagents, i.e., formamide and water (or water dimer). Electrostatic solvent effects on the geometry and properties of planar and twisted amides[40-43] and water and water dimer[34] have been examined using continuum models.

The computed electrostatic solvent effect on some molecular quantities is given in Figure 7. The geometry of formamide is slightly modified: the CN bond length decreases, whereas the CO bond length increases. This is accompanied by changes in the corresponding bond orders: the CN bond is strengthened and the CO bond is weakened. Moreover, there is a substantial polarization of the electronic charge: the absolute value of the negative charge on the oxygen and the positive charge on the hydrogen atoms bound to N increases (C and N densities are not much modified).

These effects can be rationalized by means of the usual mesomer representation if one assumes that the electronic structure is an intermediate between two electronic configurations, as represented in Chart 6. Electrostatic interactions, which generally favor charge separation, stabilize the right-hand structure. This simple interpretation must be considered with some caution since the charge transfer that it suggests is not completely satisfactory.[44]

In principle, the solvation process would be expected to disfavor nitrogen pyramidalization, since the CN double bond character increases in solution. Besides, the dipole moment is greater for the planar conformation (see below), and, following the ideas arising from Onsager's theory,[45] one expects the solute–solvent

(40) (a) Rivail, J.-L.; Rinaldi, D. In *Intermolecular Forces*; Pullman, B., Ed.; Reidel: Dordrecht, 1981; pp 343–360. (b) Dillet, V.; Rinaldi, D.; Rivail, J.-L., submitted.
(41) Burton, N. A.; Chiu, S. S. L.; Davidson, M. M.; Green, D. V. S.; Hillier, I. H.; McDouall, J. J. W.; Vincent, M. A. *J. Chem. Soc., Faraday Trans.* **1993**, *89*, 2631.
(42) Luque, F. J.; Orozco, M. *J. Chem. Soc., Perkin Trans. 2* **1993**, 683.
(43) Duben, A. J.; Miertus, S. *Chem. Phys. Lett.* **1982**, *88*, 395.
(44) Wiberg, K. B.; Breneman, C. M. *J. Am. Chem. Soc.* **1992**, *114*, 831.
(45) Onsager, L. *J. Am. Chem. Soc.* **1936**, *58*, 1486.

Table 7. Electrostatic Solvation Energies (kcal·mol^{-1}) in Water for Two Conformations of Formamide (See Text)

	cavity axes (Å)				E_{solv}[c] electrostatic			
	A	B	C	μ (D)	l = 1	l = 2	l = 3	total
planar[a]	2.018	2.674	3.442	4.114	−4.7	−1.1	−0.3	−7.5
planar[b]				4.233	−5.0	−1.1	−0.3	−13.3
pyramidal[a]	2.057	2.622	3.443	4.109	−5.2	−1.8	−0.2	−8.8
pyramidal[b]				4.141	−5.2	−1.6	−0.2	−13.8

[a] RHF/3-21G//3-1G. [b] MP2/6-31G**//3-21G. [c] Contributions to the pure electrostatic solvation energy due to the dipole (l = 1), quadrupole (l = 2), etc.

Table 8. Molecular Quantities for the TS in the Water-Assisted Neutral Reaction Mechanism as Computed in a Dielectric Continuum (ε = 78.4)

Geometrical Parameters[a]			
Bond Lengths (Å)			
CN	1.530	O_3H_1	1.120
CO_1	1.273	O_3H_2	1.098
CO_2	1.595	NH_2	1.460
O_2H_1	1.293		
Bond Angles (deg)			
O_1CN	115.26	$H_2O_3H_1$	91.26
O_2CN	97.77	O_3H_2N	150.69
H_1O_2C	109.69	H_2NC	104.69
$O_3H_1O_2$	150.11		
Dihedral Angles (deg)			
H_1O_2CN	38.76	$NH_2O_3H_1$	−4.78
$O_3H_1O_2C$	−28.31	H_2NCO_2	−35.77
$H_2O_3H_1O_2$	5.22	$H_NNCH'_N$	120.95
Total Energies (au)			
RHF/3-21G//3-21G		−319.170 041	
RHF/6-31G**//3-21G		−320.935 922	
MP2/6-31G**//3-21G		−321.859 181	
Mayer Bond Orders[33] [b]			
CN	0.796	O_3H_1	0.483
CO_1	1.440	O_3H_2	0.527
CO_2	0.549	NH_2	0.259
O_2H_1	0.279		
Mulliken Net Atomic Charges[b]			
C	0.719	O_3	−0.775
N	−0.855	H_1	0.511
O_1	−0.883	H_2	0.490
O_2	−0.816		
Dipole Moment (Debye)[b]			
6.176			

[a] At the RHF/3-31G level. [b] At the RHF/6-31G**//3-21G level.

electrostatic interaction term to favor planarity. Further computations carried out in solution for the planar and the pyramidalized structure described above show that this simple reasoning is not correct. As shown in Table 7, the pyramidalized conformation is solvated to a larger extent, so the pyramidalization energy decreases in solution (we assume cavitation and dispersion energies to remain constant in the pyramidalization process). The multipole expansion in Table 8 puts in evidence an important contribution of the quadrupole moment to the solvation energy that is substantially larger for the nonplanar molecule. Moreover, in spite of the fact that the dipole moment of the planar structure is slightly greater, its contribution to the solvation energy is slightly smaller. This is due to a change of the relative orientation of the dipole with respect to the cavity axes and must be emphasized since it illustrates the limitations of the traditional Onsager model. It should be pointed out, for completeness, that recent computations have shown rotation around the CN bond to be disfavored through the electrostatic solvent effect.[40b,41]

Bulk solvent effects on the water dimer have been discussed in detail previously.[34] The main conclusions are that the interaction increases the positive charge on the external hydrogen atoms, which are more easily available to form further hydrogen bonds with other molecules. Besides, the water dimer hydrogen bond is strengthened due to a cooperative effect of the bulk solvent and facilitates proton transfer between water molecules.

In summary, solvent effects on formamide and water dimer suggest that the reactivity of these systems would increase in solution, leading to an easier hydrolysis reaction.

(ii) Transition State TS^n. The structure of TS^n in solution is presented in Table 8. It may be compared with the corresponding structure obtained for the isolated system in Table 1. Large solvent effects are obtained: the CN and CO_2 bond lengths are substantially shorter in solution, i.e., the cleavage of the bond is retarded although the nucleophilic attack at the carbon atom is favored. Conversely, the NH_2 bond is longer in solution. Interestingly, these electrostatic solvent effects present trends similar to those reported above for acid catalysis. Nevertheless, the main geometrical change is now a large rotation of the amino group, which is made according to Chart 5b, i.e., in the direction opposite the rotation obtained in the case of the H_3O^+-promoted reaction.

(iii) Activation Energies. Solvation energies computed at the RHF/6-31G**//3-21G level are gathered in Table 9. Two components are given for each species: the pure electrostatic solvation energy, E_{elec}, defined as the free energy of interaction for the species using the gas geometry and electronic distribution, and the polarization energy, E_{pol}, which represents the stabilization due to electronic and geometry relaxation. We also give in this table the value of the gas-phase dipole moment. The electrostatic term is substantially greater for the reagents. This is essentially due to the large dipole contributions to the solvation energy of both formamide and water. Note, however, that the quadrupole contribution is quite large in TS^n. Conversely, polarization effects are larger in TS^n. It must be pointed out that polarization energies in Table 9 include the stabilization due to geometry relaxation, and our computations show that this term is substantial for TS^n. The total (electrostatic + polarization) solvation energies for the reagents and the TS^n are close, but a barrier increase (1.8 kcal·mol^{-1}) is predicted.

Table 9. Electrostatic, Polarization, and Total Solvation Energies (kcal·mol^{-1}) for the Reagents and TS in the Neutral Water-Assisted Mechanism in Water Solution at the MP2/6-31G**//3-21G Level

		ΔE_{solv} electrostatic[a]						
	μ (D)	l = 1	l = 2	l = 3	l = 4	total	polarization	total
reagents								
formamide	4.233	−6.4	−1.3	−0.3	−0.3	−8.6	−4.9	−13.5
H_2O	2.137	−3.7	−1.4	−0.1	−0.1	−5.3	−1.8	−7.1
total						−19.1	−8.6	−27.7
TS^n	3.854	−2.7	−7.7	−1.9	−1.6	−15.5	−10.4	−25.9

[a] Contributions to the pure electrostatic solvation energy due to the dipole (l = 1), quadrupole (1 = 2), etc.

One may wander what would be the effect of a moderately polar medium. The electrostatic component should always be greater for the reagents than for TS^n, but polarization effects should be less pronounced and their effect on the barrier cannot be easily predicted. Indeed, when the computations are carried out in a medium of dielectric permittivity ε = 2.0, a small increase of the barrier (~0.1 kcal·mol^{-1}) is found.

H_3O^+-Promoted Reaction. Qualitatively, the same conclusions have been obtained for the H_3O^+-promoted reaction when it is recomputed in a dielectric continuum with ε = 2.0.[46] Now the reagents are more stabilized than TS^p by 1.2 kcal·mol^{-1}, so the barrier increase is more pronounced here than in the neutral

(46) Computation in a solvent with ε = 78.4 failed to converge since the geometrical perturbation led to an open structure, the shape of which cannot be reasonably fitted by an ellipsoid.

reaction in the same medium. The electrostatic effect enhances the rotation of the amino group observed in the gas phase (Chart 5a), the H_2NCO_2 angle changing from 20.56° in a vacuum to 40.90° in a nonpolar solvent (ϵ = 2.0).

IV. Summary and Conclusions

Assistance by an ancillary water molecule renders the hydrolysis of formamide energetically more favorable in both concerted mechanisms studied in this paper, i.e., a neutral reaction and an acid-catalyzed reaction in which the carbonyl oxygen is protonated, although the effect is more important in the last case.

In the assisted processes we have found a hydrogen-bonded reaction intermediate between formamide and water which is not present in the nonassisted reactions. This can be explained through a cooperative effect in the water dimer, which is a better proton donor than the water monomer. Nevertheless, due to a substantial entropy decrease, this complex is predicted to be unstable at normal temperature and pressure conditions.

The assisted processes cannot be merely described after the nonassisted ones by simply assuming that the second water molecule solvates the system. Indeed, both water molecules strongly participate in the reaction coordinate. One important factor in considering these reactions is the greater proton donor character of the H-acceptor water molecule in the water dimer with respect to the water monomer, because it facilitates the pyramidalization of the nitrogen atom, a key feature in activating the carbon nucleophilic attack.

When electrostatic interactions with the bulk solvent are taken into account by using a continuum model for the liquid, the perturbation changes the activation barriers. However, this change is small compared to the effect of the ancillary water molecule. On the other hand, electrostatic interactions substantially modify the structure of the stationary points in the potential energy surface; therefore, in a quantitative study of the kinetics of these reactions, this effect should be taken into account.

Acknowledgment. The authors thank Professor J. Bertrán for making some interesting suggestions.